Journal of Molecular Graphics and Modelling 60 (2015) 89–97

Contents lists available at ScienceDirect

Journal of Molecular Graphics and Modelling

journal homepage: www.elsevier.com/locate/JMGM

Designing of potential inhibitors against *Staphylococcus aureus* sortase A: Combined analogue and structure based approach with *in vitro* validation

K. Kranthi Raj [a], Veeramachaneni Ganesh Kumar [b], Chalasani Leela Madhuri [b], Mathi Pardhasaradhi [b], Ravulapati Durga Lakshmi [c], M. Ravi [d], B. Sri Ramudu [a], S.V. Venkata Rao [e], D. Ramachandran [a,*]

[a] *Department of Chemistry, Acharya Nagarjuna University, Nagarjuna Nagar, Guntur 522 510, India*
[b] *Department of Biotechnology, K L E F University, Green Fields, Vaddeswaram, Guntur (Dt.), 522 502 Guntur, AP, India*
[c] *Department of Electronics and Computer Engineering, K L E F University, Green Fields, Vaddeswaram, Guntur (Dt.), 522 502 Guntur, AP, India*
[d] *Bioinformatics Division, Environmental Microbiology Lab, Department of Botany, Osmania University, Hyderabad 500 007, India*
[e] *Department of Chemistry, Rajiv Gandhi University of Knowledge Technologies, Nuzvid 521 201 AP, India*

ARTICLE INFO

Article history:
Received 3 February 2015
Received in revised form 15 May 2015
Accepted 18 May 2015
Available online 12 June 2015

Keywords:
Staphylococcus aureus sortase A
Pharmacophore modeling
Virtual screening
Indole
Thiazolidine

ABSTRACT

Staphylococcus aureus sortase A is an attractive target of Gram-positive bacteria that plays a crucial role in anchoring of surface proteins to peptidoglycan present in bacterial cell wall. Inhibiting sortase A is an elementary and essential effort in preventing the pathogenesis. In this context, *in silico* virtual screening of in-house database was performed using ligand based pharmacophore model as a filter. The developed pharmacophore model AAHR 11 consists of two acceptors, one hydrophobic and one ring aromatic feature. Top ranked molecule **KKR1** was docked into the active site of the target. After profound analysis, it was analyzed and optimized based on the observations from its binding pose orientation. Upgraded version of **KKR1** was **KKR2** and has improved docking score, binding interactions and best fit in the binding pocket. **KKR1** along with **KKR2** were further validated using 100 ns molecular dynamic studies. Both **KKR1** and **KKR2** contain Indole-thiazolidine moiety and were synthesized. The disk diffusion assay has good initial results (ZI of **KKR1**, **KKR2** were 24, 38 mm at 10 μg/mL and ZI of Ampicillin was 22 at 10 μg/mL) and calculated MICs of the molecules (**KKR1** 5.56 ± 0.28 μg/mL, **KKR2** 1.32 ± 0.12 μg/mL, Ampicillin 8 ± 1.1 μg/mL) were in good agreement with standard drug Ampicillin. **KKR1** has shown IC_{50} of 1.23 ± 0.14 μM whereas the optimized lead molecule **KKR2** show IC_{50} of 0.008 ± 0.07 μM. Results from *in silico* were validated by *in vitro* studies and proved that indole-thiazolidine molecules would be useful for future development as lead molecules against *S. aureus* sortase A.

1. Introduction

Staphylococcus aureus is a member of Firmicutes phylum and Staphylococcaceae family most of which have Gram-positive cell wall structure. The cell wall is accountable for preserving structural steadiness, providing a barrier to osmotic pressures, and assisting interactions with the surrounding environment. *S .aureus* is accountable for community and hospital acquired infections around the globe. It is predominantly responsible for the infections related to soft tissues, skin, respiratory tract and human blood stream, causing diseases impetigo, meningitis and toxic shock syndrome [1]. Amongst *S. aureus* strains, Methicillin resistant *S. aureus* (MRSA) is widespread and lethal, owing to its resistance against broad range of antibiotics [2–4]. Therefore, infections caused by this strain are key concerns of health and substantial economical tension on health care of every country. For any bacterial infection to initiate, the foremost interaction is attachment of bacterial proteins to the peptidoglycan present on the host cell wall. These anchor proteins in bacteria are pivotal for bacterial propagation and pathogenicity. In most of the Gram positive bacteria, including *S. aureus*, sortase enzymes are primarily responsible for arranging the surface proteins on the bacterial peptidoglycan for initiating the docking of bacteria on the host cell wall [5–9], showcasing them as a primary target to inhibit bacterial infections. Generally, many sortases are simple inside the identical genome and will possibly be grouped depending on their particular

* Corresponding author. Tel.: +91 7396838080.
E-mail address: dittakavirc@gmail.com (D. Ramachandran).

http://dx.doi.org/10.1016/j.jmgm.2015.05.009
1093-3263/

homology into 4 classes. Sortase A is prototypical enzyme belongs to class A family. Class B sortases usually are managed because of the accessibility to iron and anchor the proteins that will take part in heme-iron acquisition. Class C sortases have the effect of your elaboration associated with pili on bacterial surface area. Last but not least, Class D sortases usually are indicated during bacterial sporulation. Relation between different sortase proteins was explained by Thomas et al. [10] showing relationship of sortases among different bacterial species.

Out of all isoforms of sortase enzymes, sortase A is best studied and conserved among all the Gram positive bacteria with the presence of the LPXTG motif at the C-terminal of the protein. *S. aureus* sortase A enzyme (SrtA) is a extracellular cysteine transpeptidase that catalyzes a transpeptidation reaction and allows the anchorage of surface proteins to the peptidoglycan of cell wall as mentioned earlier [11]. The catalytic process or reaction occurs in two steps: (i) cysteine implicated nucleophilic attack occurs at the peptide bond between the threonine and the glycine of a conserved C-terminal motif LPXTG SrtA [12] resulting in the development of the acyl-enzyme transitional state and further covalently attaching to the peptidoglycan of the host cell membrane. The final step is the carboxyl group of the threonine connected to the amino group of the cell wall cross bridge which permits connectivity of the bacteria to host cell [13,14]. Role of cysteine present in the active site of the SrtA is evidently critical for the catalysis reaction whereas the role of other conserved amino acids Histidine and Arginine is highly controversial and imprecise. If the ability of sortase A is blocked, it prevents the anchorage of proteins present on the surface to the peptidoglycan making SrtA an attractive and significant target with superior pharmaceutical importance.

Till date, most of the inhibitors against sortase A were obtained by traditional methods, channeling the need for discovery of much effective small molecule inhibitors [15–21] by employing sophisticated computational drug discovery methods. Usage of pharmacophore modeling as a tool for the discovery of novel drugs has turned out to be progressively more popular since this method fine-tunes by considering all the aspects, leading to the discovery of novel and potent inhibitor [22]. Also, analog based pharmacophore as a filter in virtual screening is the most reliable and is comparable to its biological activity. Although, some of the researchers developed sortase A inhibitors using pharmacophore and 3D-QSAR models with only one prototype of inhibitors but, they overlook the wide range of small molecule inhibitors in the literature.

Therefore in the present study, pharmacophoric features of the inhibitors of SrtA were developed for screening Phase CAC (Commercially Available Compounds) database along with some other collection of inhibitors from our in-house database. Docking study was performed to find the right orientation of the molecule and further designed a new molecule with improved activity based on the observations. Molecular dynamics (MD) simulations were performed to find the orientation and stability of the selected molecules in the binding pocket. Molecules studied theoretically were synthesized and validated *in vitro*, which proved that the lead and fine-tuned molecules from *in silico* study were active and potent when compared to the standard drug Ampicillin.

2. Materials and methods

2.1. In silico *approaches*

2.1.1. *Ligand preparation*

The entire work was performed using MAESTRO 9.3 (Schrodinger, Inc., LLC, New York, USA), in Dell precision T3500 workstation. A dataset of 149 compounds collected from the literature [15,16,23,24]. Every compound in the data set underwent the same cell growth suppression analysis, which makes the results uniform. The dataset consists of binding data (IC_{50}) spanning over three orders of magnitude from 0.30 to 1000 μM, covering all ranges of activity from active to moderately active to inactive. All sketched compounds were imported to the project table and refined using LigPrep module [25]. OPLS_2005 (optimized potentials for liquid simulations_2005) force field was assigned to the compounds and possible states of ionization were generated using Epik [26]. Tautomers were generated and chiralities of the compound were retained. Only one low energy ring conformation was generated for each ligand. All original GI50 values of each inhibitor were converted into pGI50 (−log GI50) in order to use the data as a dependent variable.

2.1.2. *Pharmacophore model generation and database screening*

Common feature pharmacophore generation was carried out using Phase 3.1 [27] in the Maestro, a versatile product for pharmacophore perception, structure alignment and activity prediction. The workflow, building a pharmacophore model involves conformations generation with maximum 100 conformers per rotatable bond and 1000 conformers per each structure. A thorough sampling was accomplished with 100 minimization steps using OPLS_2005 force field. Distance dependent dielectric solvent treatment was considered and the maximum relative energy difference was taken as 10 kcal/mol. Redundant conformers were eliminated by setting the RMSD to 1 Å. A set of pharmacophore sites was created using pharmacophore features for all the ligands. The pharmacophore model selected was then validated by Güner-Henry (GH) scoring method, which quantifies the hits by recalling the actives from inactives from the database containing 2548 molecules. Of these 2548 molecules, 48 molecules are known inhibitors of SrtA with diverse activities. While the other 2500 are decoy molecules downloaded from the DUD decoys database (http://dude.docking.org/targets/mmp13). The decoys were used in the 1:50 ratio to find the enrichment of the developed pharmacophore model. This database with known actives and inactives was screened with the ligand and protein based pharmacophore models to calculate the GH score. The GH score has been successfully applied to quantify model selectivity, accuracy of hits and the recall of actives from a molecule dataset consisting of known actives and inactives. The GH score ranges from 0 to 1 indicating null model and ideal model, respectively.

Following is the formulae to analyze the hit lists based on ligand based pharmacophore model [28]

$$E = \frac{H_a/H_t}{A/D} \tag{1}$$

$$\mathrm{GH} = \left[\frac{H_a(3A + H_t)}{4H_tA}\right]\left[1 - \frac{H_t - H_a}{D - A}\right] \tag{2}$$

where E is the enrichment factor, GH is the goodness of hit, D is the total compounds in the dataset, A is the total number of actives in the dataset, H_t is the total hits and H_a is the active hits.

A virtual screening strategy was followed for the identification of novel SrtA inhibitors that contains a series of filters. Ligand based pharmacophore was used as filter and screening was performed against the database using the Tanimoto metric to assess similarity. Database compounds were ranked based on their similarity. Physiochemical screening (ADME) was also used as a filter.

2.1.3. *Glide ligand docking*

A GLIDE version 3.0 (Schrodinger, Inc.) in 'Extra Precision' mode (Glide XP) was used for docking [29–31] which covers all the conformations, orientations and positional space by performing a complete systematic search and eliminating unwanted conformers

using scored and followed by optimization. Further, Monte Carlo sampling of pose conformation refines the conformation. PDB-ID 2KID was considered in the study to understand ligand binding conformation and binding pattern perception. Protein retrieved from PDB was prepared with the addition of hydrogen atoms and the suitable corrections by removing water molecules and coupled with the changes related to tautomeric states of residues, orientations of hydroxyl groups, and protonation states of basic and acidic residues. The complex constraining all the heavy atoms (non-hydrogen) to their original positions with optimized hydrogen coordinates was finally minimized using OPLS_2005 force field. The protein with optimized hydrogen coordinates was finally saved as a separate file to be used for docking. The binding region was defined by a 15 Å_15 Å_15 Å box centered on the centroid of the crystal ligand to confine the centroid of the docked ligand. These residues play a key role in the direct attachment of the 2KID to the cell wall. No scaling factors were applied to the Van der Waals radii. Default settings were adopted for all the remaining factors. All the minimized compounds were docked at the active site of the target. Best pose was selected on the basis of the interactions formed between the ligands and active site amino acids and Glide score.

2.1.4. Molecular dynamic simulations

Desmond v3.1 [32] package was used to study the thermodynamically stability of the ligand–receptor complex. Predefined SPC water model was used to simulate water molecules using OPLS_2005 force field. Orthorhombic periodic boundary conditions were setup to specify the shape and size of the repeating unit. In order to neutralize the system electrically, Na^+ ions were added to balance the system charge and were placed randomly in the solvated system. After building the solvated system containing protein in complex with the ligand, the system was minimized and relaxed using default protocol integrated within Desmond. Molecular dynamic simulations were carried out with the periodic boundary conditions in the NPT ensemble. The temperature and pressure were kept at 300 K and 1 atmospheric pressure using Nose–Hoover temperature coupling and isotropic scaling; the operation was followed by running the 100 ns NPT production simulation and saving the configurations thus obtained with 5 ps intervals with a time step of 4.8 ps. All the MD runs were performed on high performance computing infrastructure (HP SL 250 2* SL250s Gen8, (2 × 2.6 GHz, 32 GB RAM, 2 × 500 GB HD, 10G IB HCA + 2 NVIDIA K20 GPU providing-4TF. Master Node). Desmond v3.1 integrated within Schrodinger platform was compiled and run under Linux CentOS 6.1 operating system.

2.5. Synthesis of screened and optimized molecule

2.5.1. General procedure for the synthesis of *KKR1* and *KKR2*

A mixture of appropriate indole-3-aldehyde (5.0 mmol), thiazolidine-2,4-dione (5.0 mmol), catalytic amount of sodium acetate (10 mg) and acetic acid (25 mL) were refluxed for 2 h at 100 °C. At the end of this period, the reaction mixture was cooled to room temperature; the separated solid was collected by filtration, washed with water (5 mL) and dried to obtain crude **KKR1** and **KKR2**. The latter, were recrystallized from EtOH to get pure **KKR1** and **KKR2**.

2.6. In-vitro

The Gram-positive strain namely, *S. aureus* (ATCC 43300) was used as test organism in screening. The cultures were diluted to achieve optical densities corresponding to 2.0×10^6 colony forming units (CFU/mL).

2.6.1. Disc diffusion assay

Equal amount of NAM (Nutrient agar medium) was poured into petri dishes, which were then dried. After solidification, a loop of culture was spread onto the media. Controls contained only Dimethyl sulfoxide (DMSO). Autoclaved paper discs containing compounds **KKR1**, **KKR2** and Ampicillin were prepared in a concentration range of 5, 10 and 15 μg/mL and were placed at different corners on the media. The plates were kept in laminar flow to enable pre-diffusion of the compounds toward the agar and were incubated overnight (18 h) at 37 °C. Ampicillin was used as positive control. Negative control was performed with discs loaded with DMSO. After the incubation period, the antibacterial activity was determined by recording the inhibition zones (IZ). Replicas at each concentration were performed.

2.6.2. Minimum inhibition concentration (MIC)

Compounds effective in zone formation were tested to determine the MIC against *S. aureus*. Compounds **KKR1**, **KKR2** and Ampicillin were prepared in a concentration range of 1, 2, 3, 4 and 5 μg/mL and tested in nutrient broth for the determination of bacterial susceptibility for *S. aureus*. The microorganism suspensions at 2×10^6 CFU/mL (colony forming unit/mL) were used to inoculate the prepared test compounds in the above mentioned serial dilution broth. The culture tubes were incubated at 37 °C for 24–48 h. At the end of the incubation period, the growth of bacteria was estimated with turbidity measurements. The MIC is defined as the lowest concentration that showed no bacterial growth.

2.6.3. FRET assay

Hit from virtual screening and optimized lead molecule were tested for their inhibition capabilities. Fluorescence resonance energy transfer (FRET) assay was performed to measure activity of molecules against $SrtA_{\Delta N59}$ protein. Experimental procedure used, as described in the literature. [33] Fluorescence was measured, and an estimate of the relative units of $SrtA_{\Delta N59}$ activity per mL was calculated. IC_{50} values were calculated by measuring the three independent sets of data using the following equation:

$$\left[\frac{V_i}{V_0}\right] = \left[\frac{1}{1 + \left[[I]/IC_{50}\right]^h}\right] \quad (3)$$

where V_i and V_0 are initial velocity of the reaction in the presence and absence of an inhibitor of concentration [I], respectively. The term h is Hill's coefficient.

3. Results and discussion

The main goal of the study is to discover a novel and potent hit that can inhibit SrtA and impede the ability of protein anchoring the surface proteins to peptidoglycan present in bacterial cell wall. The availability of lesser number of potential hits and the need for the more actions chemo types for inhibiting Gram positive bacteria are the major reasons to initiate this study. Fig. 1 depicts the workflow executed in the study. In the current work, PHASE module of Maestro Suite was engaged to generate common feature pharmacophore model, which was based on all SrtA inhibitors available in the literature. The generated pharmacophore model was used as a main filter to screen the in-house database that contains a collection of some chemo types along with phase database. Screened molecules were docked into the active site of the SrtA for identifying its orientation and binding pattern.

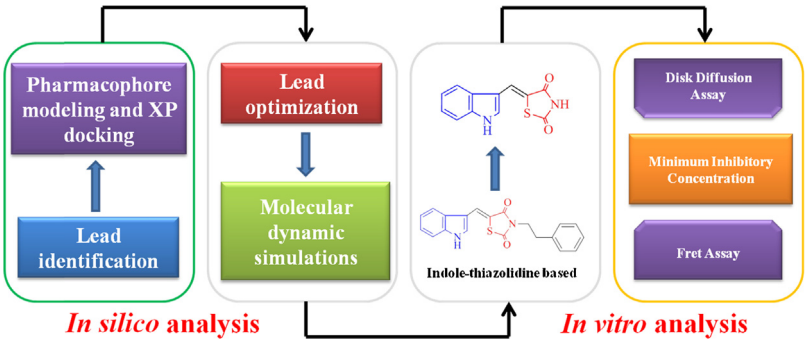

Fig. 1. Flow chart dipicting the work flow of current study.

3.1. Pharmacophore model generation, validation and screening

Ligand based drug discovery approach was used to find the novel hits. All the experimental values were changed to their respective log values for the convenience. Total number of ligands used in the study was 149. A threshold limit was set to pIC_{50} value $\leq$5 for inactives and pIC_{50} value $\geq$6 for actives and remaining all were considered moderately active. The above filter resulted in 21 active, 59 inactive and 69 moderately active molecules. A common feature pharmacophore was developed using 18 actives by a tree based partition algorithm with maximum tree depth of five. 26 four featured pharmacophore hypotheses from the variant list were generated. Rigorous scoring analysis was performed to rank the generated common feature pharmacophore hypotheses and was listed in Supplementary Table 1. Pharmacophore hypothesis AAHR11 was selected as the best because of its highest survival score = 3.77. Pharmacophoric features present in this hypothesis contain one hydrogen bond acceptor, one hydrophobic and two ring aromatic regions and were shown in Fig. 2.

The quality of the common feature pharmacophore hypotheses was observed based on the fitness scores of the ligands used in generating the model. AAHR11 has the highest fitness score 3.00 with the most active molecule of the dataset and has a lowest score of 1.25 with the least active molecule. It was observed AAHR11 has all the features that match with the most active molecule, and it has only two features out of four that match with the least active molecule. This indicates that pharmacophore model is competent to pick the actives rather than inactives from the database. The efficiency and superiority of the model was further validated using the GH scoring method. Validation was done using different types of parameters like total hits (H_t), active hits (H_a), percent yield of actives ($H_a/H_t \times 100$), percent ratio of actives ($H_a/A \times 100$), the enrichment factor (EF) and goodness of hit score or Guner–Henry score (GH). Pharmacophore model AHRR33 was successful in retrieving the 93.33% active compounds. In addition, the calculated EF and GH scores for common feature pharmacophore are found to be 36.98 and 0.752, respectively, which indicate the quality of pharmacophore model was similar to standard. From this validation, it was clear that the model was significant and has substantial supremacy to differentiate actives from inactives in the database.

Generated database was screened using the 3D-pharmacophore hypothesis (AAHR11) using the default screening protocol of Phase software. Top 5 molecules were ranked according to their scores based on the fitness to the given hypothesis. Scores along with the ligands matched on 3D-pharmacophore were analyzed (Supplementary Fig. 1). Out of all, the high ranked molecule contains indole and thiazolidine rings as a core moiety. Further after screening, molecules passed the ADME filter, a physiochemical filter, suggesting that these molecules can go further into the drug discovery pipeline without later phase decline.

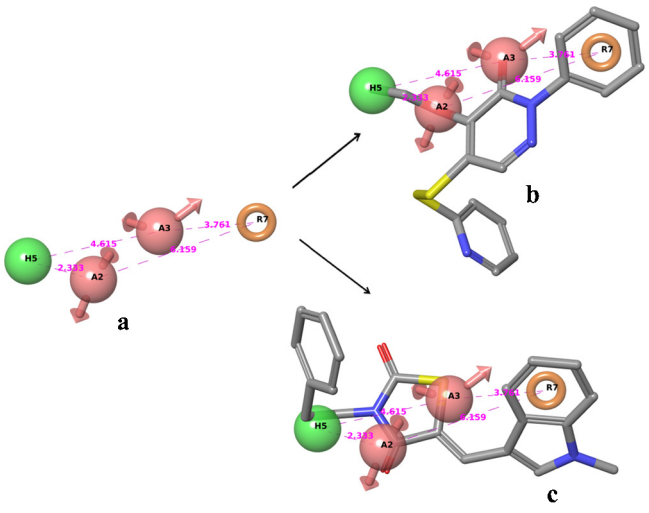

Fig. 2. (a) Common feature pharmacophore generated from the selected ligands from the literature. (b) Most active compound used in the generation of common feature pharmacophore. (c) Virtual hit picked from the virtual screening using common feature pharmacophore. (For interpretation of the references to color in this figure legend, the reader is referred to the web version of this article.)

3.2. Docking

The extra precision docking protocol was validated by redocking the co-crystallized ligand present in its respective binding site. Redocked ligand has reproduced the same binding pose as the native along with a good docking score of −8.79 and the RMSD between the native ligand conformation and the redocked one was 0.21 Å. It was observed that the above protocol retained the native pose and hence can be employed to identify the correct binding pose for novel hits. Top 5 molecules obtained from screening protocol were docked into the protein active site and were ranked again based on the interaction with the amino acid residues and docking scores. It is interesting to discover that the same molecule **KKR1** was ranked top in both screening and glide XP docking. Docking results were tabulated in Table 1 and Fig. 3 depicts the binding orientation of the top ranked molecule **KKR1**.

All the known active molecules used for developing the pharmacophore were docked into active site of 2KID and have shown the same pattern of binding orientation (Supplementary Fig. 2) and no molecule has shown interactions with all the three important amino acids present in the binding pocket. After that molecule **KKR1** was profoundly analyzed due to its merit in both the protocols used in this study. IUPAC

Table 1
In silico results of **KKR1**, **KKR2** and Ampicillin along with their ADME properties.

Compound Name	**KKR1**	**KKR2**	Ampicillin
Hydrophobic network (within 5 Å)	Ala 92, Leu97, Ala 104, Ala 118, Val 116, Pro 163, Val 166, Val 168, Ile 182, Cys 184, Val 193	Ala 92, Leu97, Ala 104, Ala 118, Val 116, Pro 163, Val 166, Val 168, Ile 182, Cys 184	Pro 91, Ala 92, Leu97, Ala 104, Ile 117, Ala 118, Ile 182, Cys 184
H-bond interaction	Arg197, NH—O	Arg197, NH—O 1.94 Å His120, N—HNO 2.14 Å Cys184, NH—O	–
Glide score	−6.96	−8.26	−5.56
ZI (mm) at 10 μg/mL	10.0	28.0	22.0
MIC (μg/mL)	5.56 ± 0.28	1.32 ± 0.12	8 ± 1.1
IC_{50} (μM)	1.23 ± 0.14	0.008 ± 0.07	–
QPlogPo/w[1]	5.3	2.2	−1.9
QPlogS[2]	−6.1	−3.6	−1.5
QPPCaco[3]	1796.1	309.5	3.3
QPPMDCK[4]	1370.6	574.9	5.1
Percent human oral absorption[5]	100.0	84.0	24.0

[1] Predicted octanol/water partition coefficient (recommended range −2.0 to 6.5).
[2] Predicted aqueous solubility, log *S*. *S* in mol/dm^3 in the concentration of the solute in a saturated solution that is in equilibrium with the crystalline solid (recommended range −2.0 to 6.5).
[3] Predicted apparent Caco-2 cell permeability in nm/s (recommended range <25 poor to >500 great).
[4] Predicted apparent MDCK cell permeability in nm/s (recommended range <25 poor to >500 great).
[5] Percentage of human oral absorption (recommended range <25% poor to >80% high).

name of **KKR1** was (*Z*)-5-((1-methyl-1*H*-indol-3-yl) methylene)-3-phenethylthiazolidine-2,4-dione. Important amino acids present in the binding pocket are His 120, Arg 197 and Cys 184. Keto group attached to thiazolidine in **KKR1** has shown hydrogen bond with Arg 197 (O—HN, 2.38 Å) and indole and phenyl ring has shown π-cation, π–π interactions with the same amino acid Arg 197. Since non bonded interactions like hydrogen bond, π-cation, π–π stacking play a crucial role in the binding of molecules to the target protein, **KKR1** can show good activity against SrtA. In our previous work, molecules that have shown interactions with Arg 197 and His 120 were given importance and they were proven to be active in vitro as well. Our main aim in this work as mentioned earlier was to design a better molecule than the previous molecules reported from our lab. A molecule that can show interactions with all the conserved amino acids His 120, Arg 197 and Cys 184, can only show good activity against target.

For even better binding, **KKR1** molecule was further optimized by adding and deleting groups. **KKR1** was mapped against the binding site of SrtA and its fitting in the pocket was analyzed. Based on the observations, it was clear that the phenyl group attached to thiazolidine ring through an alkyl chain was not accommodated appropriately in the binding pocket, which was responsible for the increase in the penalty for not fitting well into the binding pocket. Another observation was that, there is no other group in the molecule that can donate hydrogen to proximate amino acid His 120 to form a hydrogen bond which is one of the prerequisites for designing best molecule. If phenyl ring along with alkyl chain was knocked, the solutions for both the problems mentioned above can be achieved. Methyl group attached to indole ring can be removed because it's non-involvement in binding of the molecule and its presence could be a problem for fitting of molecule in the binding pocket. The overall fit of the molecule could be enhanced if the observed space above the indole was filled with an appropriate functional group.

Considering all the observations, optimization of **KKR1** was performed. Removal of the phenyl group and alkyl chain lead to the best fit of the molecule in the binding pocket without penalties and also the nitrogen present in thiazolidine of the molecule has formed hydrogen bond with Arg 197 (NH—N, 2.35 Å). Along with the two changes, one more interaction with the molecule was observed with Cys 184 (O—HN, 2.75 Å), which was considered as an added advantage as this was the key problem that should be addressed after the problem of penalty for over fitting the molecule in the binding pocket. Due to the knocking of groups attached to thiazolidine, the dihedral angle between the indole and thiazolidine was transformed from 169.1° to 178.4° allowing it to form a hydrogen bond with Cys 184. Deletion of methyl group and addition of bromide to the indole ring has increased the fitness of molecule in the binding pocket. All the observations were implemented on **KKR1** to fine-tune the glitches and the new ligand was labeled as **KKR2** (IUPAC name is (*Z*)-5-((5-bromo-1*H*-indol-3-yl) methylene) thiazolidine-2, 4-dione). To testify the fine-tuning process, **KKR2** was docked into the active site of 2KID and tremendous change was observed in docking score, binding interactions and alignment of molecule in the binding site. Docking score was improved to −10.26 with enhanced hydrogen bond network forming bonds with His 120, Arg 197 and the most important Cys 184. Fig. 4 shows the interactions formed due to the change in functional groups to **KKR1** and Fig. 5 shows the binding pose orientation of **KKR1** and **KKR2** in the active site.

Supplementary Fig. 3 shows the binding orientation of standard drug Ampicillin. As already known, the drugs used at present were not developed based on the target information and so it has no interaction with the main amino acids present in the binding pocket even though they have shown a weak π-cation and salt bridge with Arg 197. Thus much information cannot be rendered from the docking of standard drug Ampicillin. Unregulated use of antibiotics in clinic increased the emergence of antibiotic resistant strains. Problem of resistance to the standard drugs, especially MSRA (Methicillin resistant *S. aureus*) was to be considered while developing or designing new drugs. Designing drugs against resistant strains was a challenge and this problem can be solved by working with SrtA as its gene was found to be intact in mutant population of *S. aureus*. In other words targeting SrtA genes will also address the resistance problem.

3.3. Molecular dynamic simulations

Optimization was followed by 100 ns Molecular dynamic simulations to understand the difference in stability between **KKR1** and **KKR2** in complex with 2KID by comparing with Ampicillin as a standard. For the complex Ampicillin-2KID, the total energy was unstable throughout the simulation fluctuating between

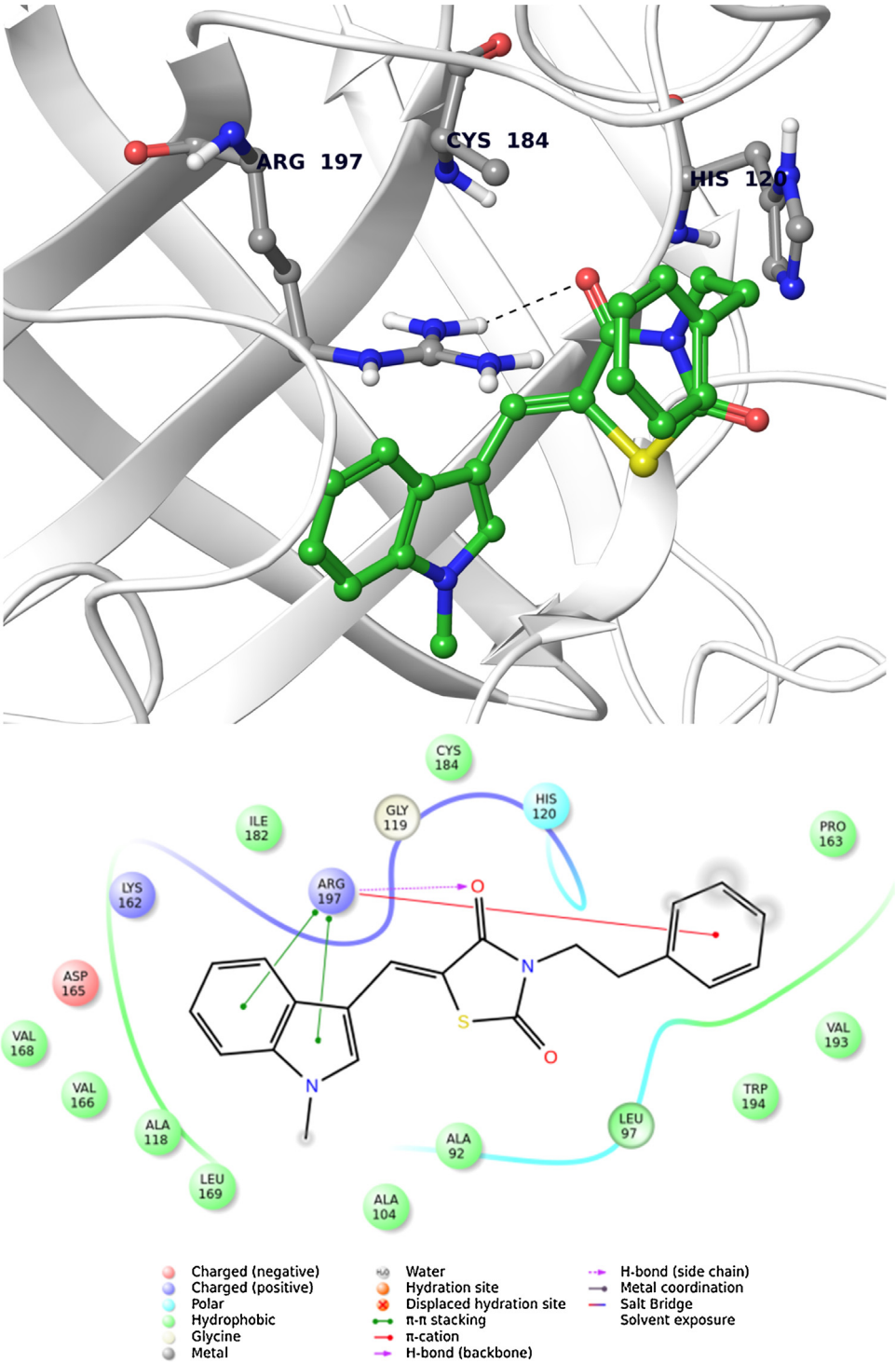

Fig. 3. Top ranked molecule **KKR1** (green) from ligand based pharmacophore studies. (For interpretation of the references to color in this figure legend, the reader is referred to the web version of this article.)

50 and −100 kcal/mol. On the other hand, **KKR1** and **KKR2** have attained stability in total energy by 5 ns of the run. Also, when compared between **KKR1** and **KKR2**, the energy of the former ranged between −100 and −200 kcal/mol and the latter from −200 to −250 kcal/mol indicating the stability of the ligands in the active site followed the order of **KKR2** > **KKR1** > Ampicillin (Fig. 6). Even though Ampicillin is a standard drug for the Gram positive bacteria, results suggest its decreased specificity against SrtA as it is unable to fit into the active site during the simulation. Also, the change in binding poses between Ampicillin and **KKR2**, **KKR1** correlates to the change in the energy differences and this evidently proves that the molecules designed in this study were more accommodating in the active site of the protein.

C-alpha RMSD was analyzed for all the frames with respective to the initial frame. Ampicillin has shown maximum RMSD fluctuations ranging between 2 to 5 Å but **KKR1** and **KKR2** proved to very stable with less RMSD fluctuations around 2 Å (Fig. 7). RMSF

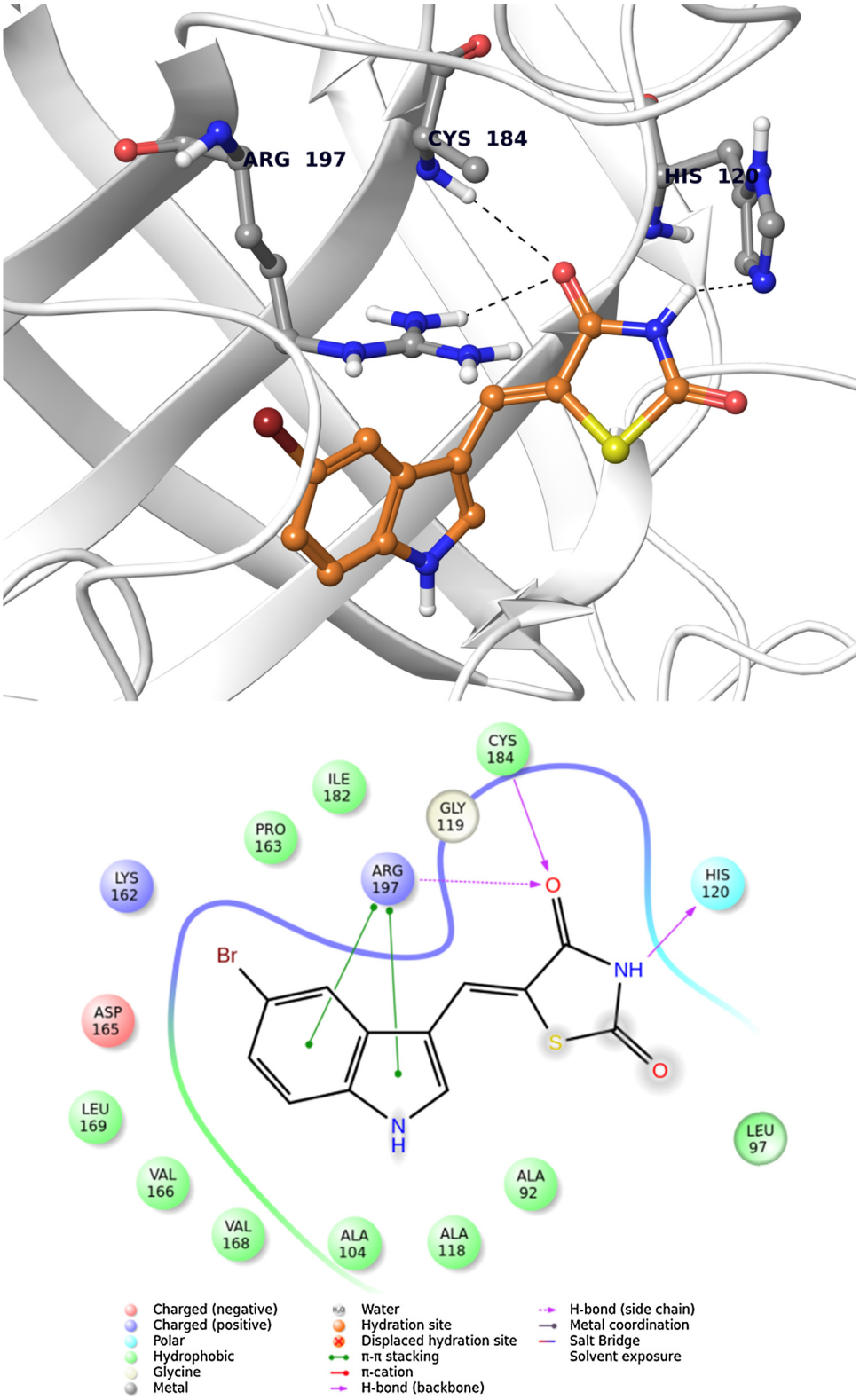

Fig. 4. Optimized molecule **KKR2** (orange) from the binding pattern analysis. (For interpretation of the references to color in this figure legend, the reader is referred to the web version of this article.)

of C-alpha amino acids of the compounds **KKR1** and **KKR2** along with Ampicillin was evaluated and evidenced that **KKR1** and **KKR2** have fewer fluctuations around 2 Å (Supplementary Fig. 4), while amino acids of protein in complex with Ampicillin have shown mighty fluctuations reaching up to 10 Å during the total trajectory. From MDS, it was clear that the **KKR1** and **KKR2** were more stable than the standard drug Ampicillin and due to this reason, these molecules were synthesized and elucidated using NMR and MASS (Supplementary Figs. 5–8) further validated using *in vitro* studies.

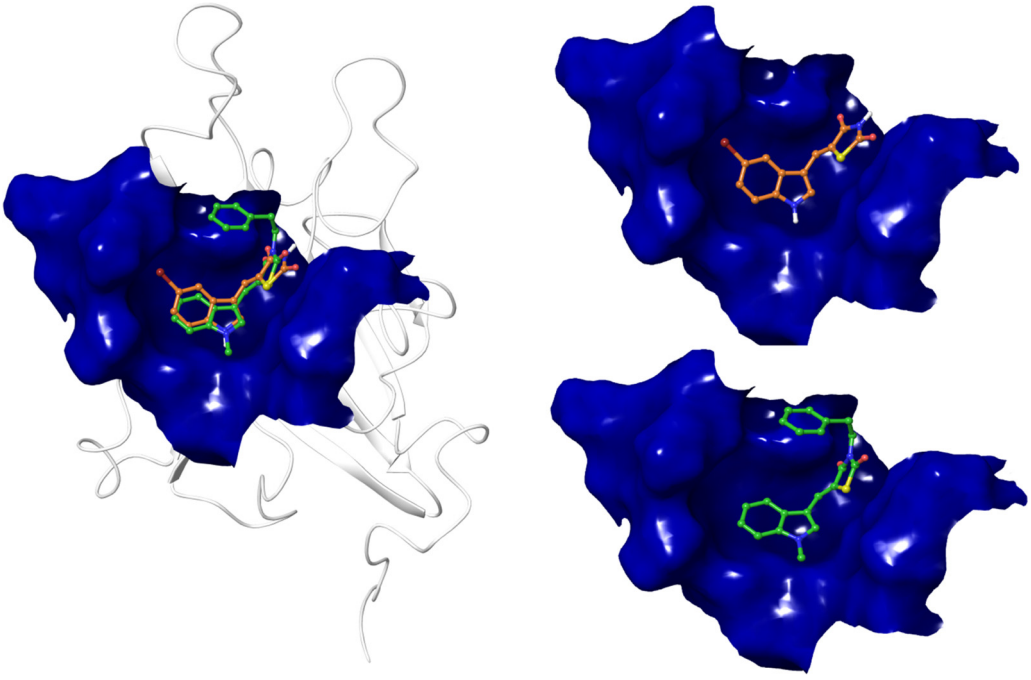

Fig. 5. **KKR1** and **KKR2** in the bindpocket of 2KID. Blue color represents the binding pocket of 2KID protein. Green color molecule is **KKR1** and orange color molecules is **KKR2**. (For interpretation of the references to color in this figure legend, the reader is referred to the web version of this article.)

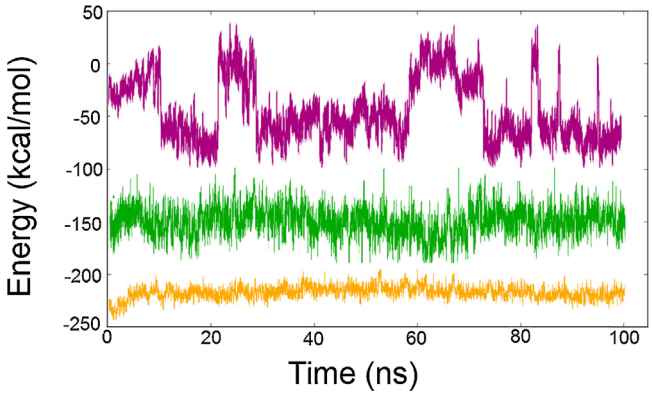

Fig. 6. Calculated total energy throughout the MD trajectory simulation time of 100 ns of SrtA in complex with Ampicillin (maroon), **KKR1** (green) and **KKR2** (orange). (For interpretation of the references to color in this figure legend, the reader is referred to the web version of this article.)

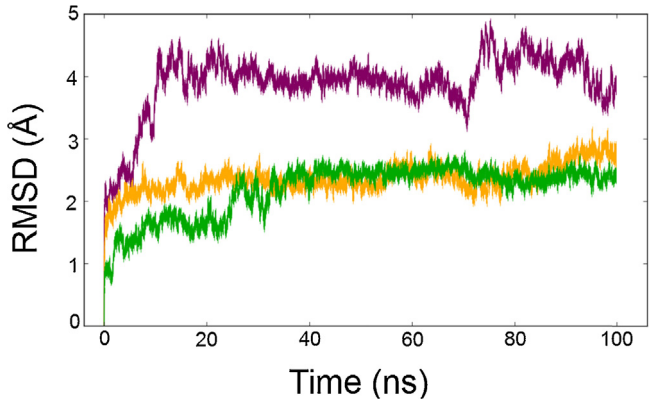

Fig. 7. Calculated RMSD throughout the MD trajectory simulation time of 100 ns of SrtA in complex with Ampicillin (maroon), **KKR1** (green) and **KKR2** (orange). (For interpretation of the references to color in this figure legend, the reader is referred to the web version of this article.)

KKR1: IR (KBr): 1735 and 1645 cm^{-1} (both s, sharp, two —C=O groups); ^1H NMR (400 MHz, DMSO-d_6/TMS): δ 3.94 (s, 3*H*, —CH_3), 4.74 (s, 2*H*, —NCH_2 of benzyl (TZD)), 7.25–8.20 (m,11*H*, 9*H* aromatic benzyl + 1*H* vinylic proton + 1*H* α-indolyl); Anal. Calcd. for ($C_{20}H_{16}N_2O_2S$) requires C,68.94; H, 4.63; found C,68.91; H, 4.59%; CIMS: *m/z* ($M^+ + 1$): 349.

KKR2: IR (KBr): 3559, 3515 cm^{-1} (broad, medium, two —NH groups), 1758 and 1648 cm^{-1} (both s, sharp, two —C=O groups); ^1H NMR (400 MHz, DMSO-d_6/TMS): δ 7.57–8.57 (m, 5*H*, 3*H* indole aromatic + 1*H* α-indolyl + 1*H* vinylic proton), 12.26–12.53 (s, 2*H*, two —NH, D_2O exch); $C_{12}H_7BrN_2O_2S$, Analysis Calcd. for C, 44.60; H, 2.18; N, 8.67, Found: C, 44.70; H, 2.38; N, 8.87; CIMS: *m/z* ($M^+ + 1$): 322.

3.4. Determination of biological activity

Only **KKR1** and **KKR2** molecules were considered for *in vitro* screening along with standard Ampicillin. At 5, 10, 15 μg/mL, **KKR1** has shown IZ of 6, 10, 15 mm and **KKR2** has IZ of 10, 28, 38 mm in diameter, respectively. At higher concentration (15 μg/mL), **KKR1** has shown similar activity when compared to Ampicillin, but at 10 μg/mL concentration, Ampicillin was better than **KKR1**. However, **KKR2** at 10 μg/mL has higher IZ than standard. Since the experiment was dose dependent, higher concentration of **KKR2** has drastically increased the zone. Although **KKR1** and **KKR2** were showing activity at minimum dose 5 μg/mL, there is still a requirement to speculate the exact MICs of these molecules. The MICs of 2 compounds against test organism *S. aureus* were evaluated along with the standard and were represented in Table 1 and Supplementary Fig. 9 shows the zone of inhibition in petri plates. **KKR1** has shown MIC of 5.56 ± 0.28 μg/mL where as **KKR2** has lower MIC of 1.32 ± 0.12 μg/mL compared with Ampicillin, while **KKR2** has significant MIC and IZ that exceeded the range of Ampicillin (8 ± 1.1 μg/mL). Inhibitory concentrations of compounds were measured using a FRET-based assay. Compound **KKR1** has shown IC_{50} of 1.23 ± 0.14 μM whereas the optimized lead molecule **KKR2** shown IC_{50} of 0.008 ± 0.07 μM. This result

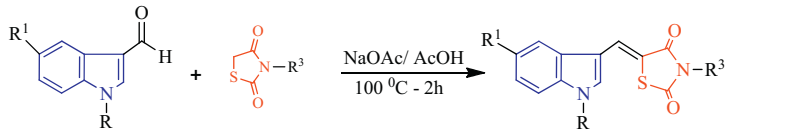

KKR1 - R-CH_3, R^1-H, R^3- $CH_2CH_2C_6H_5$
KKR2 - R-H, R^1-Br, R^3-H

Scheme 1. Scheme for the synthesis of molecules **KKR1** and **KKR2**.

enumerates the efficiency of the protocol used in the drug discovery process.

4. Conclusion

Pharmacophore modeling for the SrtA inhibitors was performed and four featured pharmacophore hypotheses were developed. A four point pharmacophore with 1 hydrogen bond acceptor, 1 hydrophobic feature and two rings aromatic with a high survival score were predicted. The developed ligand based pharmacophore model was validated using the GH scoring method. The ligand based pharmacophore model was successful in retrieving the 95% of active compounds from the decoys set. This pharmacophore hypothesis is further used to screen the in-house database for the identification of potential SrtA inhibitor **KKR2**. From *in silico* studies, compound **KKR1** was found to have a good glide score and binding free energy of −53.28 kJ/mol. Hit obtained from screening was optimized to **KKR2** and was validated with 100 ns MDS to have stable interactions with binding site amino acids when compared with the known standard. The inhibitory action of the compound **KKR2** was tested *in vitro* using Disk diffusion, MIC and IC_{50} values and has shown good results. We speculate that the inhibition of SrtA in *S. aureus* could be one of the targets for antibacterial function, and thus provided the molecular basis for the development of **KKR2** as a novel agent against anti-bacterial infections (Scheme 1).

Appendix A. Supplementary data

Supplementary data associated with this article can be found, in the online version, at http://dx.doi.org/10.1016/j.jmgm.2015.05.009

References

[1] K.B. Oh, K.W. Nam, H. Ahn, J. Shin, S. Kim, W. Mar, Therapeutic effect of (*Z*)-3-(2,5-dimethoxyphenyl)-2-(4-methoxyphenyl) acrylonitrile (DMMA) against *Staphylococcus aureus* infection in a murine model, Biochem. Biophys. Res. Commun. 396 (2010) 440–444.
[2] H.C. Baggett, T.W. Hennessy, K. Rudolph, D. Bruden, A. Reasonover, A. Parkinson, et al., Community-onset methicillin-resistant *Staphylococcus aureus* associated with antibiotic use and the cytotoxin Panton-Valentine leukocidin during a furunculosis outbreak in rural Alaska, J. Infect. Dis. 189 (2004) 1565–1573.
[3] S. Deresinski, Methicillin-resistant *Staphylococcus aureus*: an evolutionary, epidemiologic, and therapeutic odyssey, Clin. Infect. Dis. 40 (2005) 562–573 (an official publication of the Infectious Diseases Society of America.).
[4] D. Salerno, B. Vahid, P.E. Marik, Methicillin-resistant *Staphylococcus aureus* pneumonia after thoracic surgery: successful treatment with linezolid after failed vancomycin therapy, Ann. Thorac. Surg. 83 (2007) 1888–1891.
[5] L.A. Marraffini, A.C. Dedent, O. Schneewind, Sortases and the art of anchoring proteins to the envelopes of gram-positive bacteria, Microbiol. Mol. Biol. Rev.: MMBR 70 (2006) 192–221.
[6] S.K. Mazmanian, G. Liu, H. Ton-That, O. Schneewind, *Staphylococcus aureus* sortase, an enzyme that anchors surface proteins to the cell wall, Science (New York, N.Y.) 285 (1999) 760–763.
[7] G.K. Paterson, T.J. Mitchell, The biology of Gram-positive sortase enzymes, Trends Microbiol. 12 (2004) 89–95.
[8] H. Ton-That, G. Liu, S.K. Mazmanian, K.F. Faull, O. Schneewind, Purification and characterization of sortase, the transpeptidase that cleaves surface proteins of *Staphylococcus aureus* at the LPXTG motif, Proc. Natl. Acad. Sci. U.S.A. 96 (1999) 12424–12429.
[9] H. Ton-That, L.A. Marraffini, O. Schneewind, Protein sorting to the cell wall envelope of Gram-positive bacteria, Biochim. Biophys. Acta 1694 (2004) 269–278.
[10] Thomas Spirig, E.M. Weiner, R.T. Clubb, Sortase enzymes in Gram-positive bacteria, Mol. Microbiol. 82 (2011) 1044–1059.
[11] A.M. Perry, H. Ton-That, S.K. Mazmanian, O. Schneewind, Anchoring of surface proteins to the cell wall of *Staphylococcus aureus*. III. Lipid II is an in vivo peptidoglycan substrate for sortase-catalyzed surface protein anchoring, J. Biol. Chem. 277 (2002) 16241–16248.
[12] O. Schneewind, P. Model, V.A. Fischetti, Sorting of protein A to the staphylococcal cell wall, Cell 70 (1992) 267–281.
[13] M.L. Bentley, H. Gaweska, J.M. Kielec, D.G. McCafferty, Engineering the substrate specificity of *Staphylococcus aureus* Sortase A. The beta6/beta7 loop from SrtB confers NPQTN recognition to SrtA, J. Biol. Chem. 282 (2007) 6571–6581.
[14] X. Huang, A. Aulabaugh, W. Ding, B. Kapoor, L. Alksne, K. Tabei, et al., Kinetic mechanism of *Staphylococcus aureus* sortase SrtA, Biochemistry 42 (2003) 11307–11315.
[15] A.H. Chan, J. Wereszczynski, B.R. Amer, S.W. Yi, M.E. Jung, J.A. McCammon, et al., Discovery of *Staphylococcus aureus* sortase A inhibitors using virtual screening and the relaxed complex scheme, Chem. Biol. Drug Des. 82 (2013) 418–428.
[16] B.C. Chenna, J.R. King, B.A. Shinkre, A.L. Glover, A.L. Lucius, S.E. Velu, Synthesis and structure activity relationship studies of novel *Staphylococcus aureus* Sortase A inhibitors, Eur. J. Med. Chem. 45 (2010) 3752–3761.
[17] K.M. Connolly, B.T. Smith, R. Pilpa, U. Ilangovan, M.E. Jung, R.T. Clubb, Sortase from *Staphylococcus aureus* does not contain a thiolate-imidazolium ion pair in its active site, J. Biol. Chem. 278 (2003) 34061–34065.
[18] M.E. Jung, J.J. Clemens, N. Suree, C.K. Liew, R. Pilpa, D.O. Campbell, et al., Synthesis of (2R,3S) 3-amino-4-mercapto-2-butanol, a threonine analogue for covalent inhibition of sortases, Bioorg. Med. Chem. Lett. 15 (2005) 5076–5079.
[19] R.G. Kruger, S. Barkallah, B.A. Frankel, D.G. McCafferty, Inhibition of the *Staphylococcus aureus* sortase transpeptidase SrtA by phosphinic peptidomimetics, Bioorg. Med. Chem. 12 (2004) 3723–3729.
[20] C.K. Liew, B.T. Smith, R. Pilpa, N. Suree, U. Ilangovan, K.M. Connolly, et al., Localization and mutagenesis of the sorting signal binding site on sortase A from *Staphylococcus aureus*, FEBS Lett. 571 (2004) 221–226.
[21] C.J. Scott, A. McDowell, S.L. Martin, J.F. Lynas, K. Vandenbroeck, B. Walker, Irreversible inhibition of the bacterial cysteine protease-transpeptidase sortase (SrtA) by substrate-derived affinity labels, Biochem. J. 366 (2002) 953–958.
[22] S. Kalva, E.R. Azhagiya Singam, V. Rajapandian, L.M. Saleena, V. Subramanian, Discovery of potent inhibitor for matrix metalloproteinase-9 by pharmacophore based modeling and dynamics simulation studies, J. Mol. Graphics Modell. 49 (2014) 25–37.
[23] B.C. Chenna, B.A. Shinkre, J.R. King, A.L. Lucius, S.V. Narayana, S.E. Velu, Identification of novel inhibitors of bacterial surface enzyme *Staphylococcus aureus* Sortase A, Bioorg. Med. Chem. Lett. 18 (2008) 380–385.
[24] N. Suree, S.W. Yi, W. Thieu, M. Marohn, R. Damoiseaux, A. Chan, et al., Discovery and structure-activity relationship analysis of *Staphylococcus aureus* sortase A inhibitors, Bioorg. Med. Chem. 17 (2009) 7174–7185.
[25] Small-Molecule Drug Discovery Suite 2014-1, 2014.
[26] J.C. Shelley, A. Cholleti, L.L. Frye, J.R. Greenwood, M.R. Timlin, M. Uchimaya, Epik: a software program for p*K*(a) prediction and protonation state generation for drug-like molecules, J. Comput.-Aided Mol. Des. 21 (2007) 681–691.
[27] S.L. Dixon, A.M. Smondyrev, S.N. Rao, PHASE: a novel approach to pharmacophore modeling and 3D database searching, Chem. Biol. Drug Des. 67 (2006) 370–372.
[28] W. Tai, T. Lu, H. Yuan, F. Wang, H. Liu, S. Lu, et al., Pharmacophore modeling and virtual screening studies to identify new c-Met inhibitors, J. Mol. Model. 18 (2012) 3087–3100.
[29] R.A. Friesner, R.B. Murphy, M.P. Repasky, L.L. Frye, J.R. Greenwood, T.A. Halgren, et al., Extra precision glide: docking and scoring incorporating a model of hydrophobic enclosure for protein–ligand complexes, J. Med. Chem. 49 (2006) 6177–6196.
[30] Glide, version 6.2, Schrödinger, LLC, New York, NY, 2014.
[31] T.A. Halgren, R.B. Murphy, R.A. Friesner, H.S. Beard, L.L. Frye, W.T. Pollard, et al., Glide: a new approach for rapid, accurate docking and scoring. 2. Enrichment factors in database screening, J. Med. Chem. 47 (2004) 1750–1759.
[32] Y. Shan, M.A. Seeliger, M.P. Eastwood, F. Frank, H. Xu, M.O. Jensen, et al., A conserved protonation-dependent switch controls drug binding in the Abl kinase, Proc. Natl. Acad. Sci. U.S.A. 106 (2009) 139–144.
[33] H. Ton-That, S.K. Mazmanian, K.F. Faull, O. Schneewind, Anchoring of surface proteins to the cell wall of *Staphylococcus aureus*. Sortase catalyzed in vitro transpeptidation reaction using LPXTG peptide and NH(2)-Gly(3) substrates, J. Biol. Chem. 275 (2000) 9876–9881.